Achieving axial fan sound reduction with micro-perforated absorbers

Sebastian Floss[1], Felix Czwielong[2], Florian Krömer[2], Stefan Becker[2], Manfred Kaltenbacher[1]
[1] *Institut für Mechanik und Mechatronik E325-3 Technische Akustik, TU Wien, Österreich*
[2] *Lehrstuhl für Prozessmaschinen und Anlagentechnik (iPAT), FAU Erlangen-Nürnberg, Deutschland*

Introduction

The usage of micro-perforated absorbers (MPA) in HVAC duct scenarios has been shown [1] to reduce the emitted sound power significantly. So far, purely acoustic measurements without a stationary volume flow rate have been conducted. The underlying acoustic mechanism of a flush mounted MPA liner arrangement makes use of cross section jumps and cavities which can have a detrimental effect on the pressure drop and overall performance of a fluid flow engine. In this contribution we therefore investigate experimentally the effect of such a liner on the performance of an axial fan in a duct arrangement. The fan's efficiency, pressure drop and overall sound emission at several operating points are evaluated. We study emitted sound spectra to assess the MPA's impact on sound pressure level (SPL) reduction.

Basal MPA

A micro-perforated absorber consists of a micro-perforated plate (MPP) in front of a sound hard wall. Wave energy is dissipated in the sub-millimeter perforation of the plate, characterized by the perforation rate ϕ and specific flow resistivity σ. The wall is recessed from the MPP by a length D (see Figure 1). If the sound waves impinge on the plates, the variation of length D allows to select a specific target frequency (for D in the range of $\lambda/4$, with λ as the wave length) band with large energy dissipation. Simulations and measurements of different MPP arrangements in an expansion chamber without flow [1] show that a cross section jump effect on sound power reduction can also be augmented by MPPs. In this case, the sound waves impinge on the MPP in a grazing incident angle (see Figure 2). By changing the back volume length of the MPP in axial direction, one can tackle specific lower frequency bands (<1500 Hz). In this case, the variation of length D determines the cross section ratio and therefore the maximum sound pressure amplitude reduction.

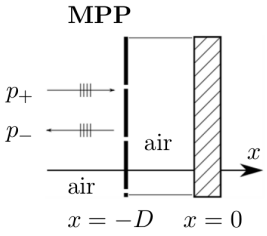

Figure 1: Basal MPA configuration with micro-perforated plate (MPP) and cavity length D.

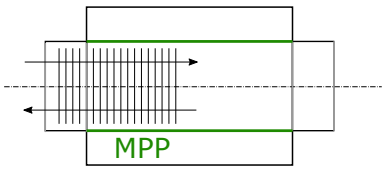

Figure 2: Expansion chamber arrangement, plane sound wave fronts impinging on MPP in grazing incident angle

Fan duct arrangement

The typical sound emission spectrum of an axial fan with differently skewed blade geometry running near the in-flow nozzle of a duct is shown in Figure 3. One can distinguish tonal components at the blade passage frequency and its harmonics caused by in-stationary flow phenomena and distorted in-flow conditions, and a broadband high amplitude SPL (sound pressure level) at frequencies below 1000 Hz is visible.
The MPA was therefore designed to reduce the sound emission below 1000 Hz. The plate material is 0.5 mm thick stainless steel with slit-shaped perforations (Acoustimet^{TM}, SONTECH) bended to a diameter of roughly 506 mm. The length of the liner L is 440 mm and the cavity length D = 137 mm (see Figure 4). In one scenario the fan (diameter of 495 mm) runs above the MPP (SII in Figure 4). Here, perfusion of the MPP in radial direction is possible and the larger diameter of 506 mm in comparison to the substituting (subs) solid metal tube's diameter of 500 mm results in a larger tip gap of 5.5 mm (2.5 mm for the substitute metal tube). To avoid this perfusion and the change in aeroacoustically induced noise and aerodynamical fan performance due to the larger tip gap, a second position of the fan was investigated (SIII in Figure 5). Here, the fan runs above a solid metal duct section with the same tip re-

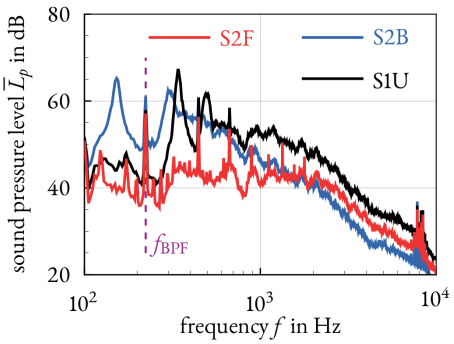

Figure 3: Sound emission of fan with different blade geometries (see Figure 6) [2] at 1.4 m^3s^{-1}, blade passage frequency f_{BPF}, S1U blades are unskewed.

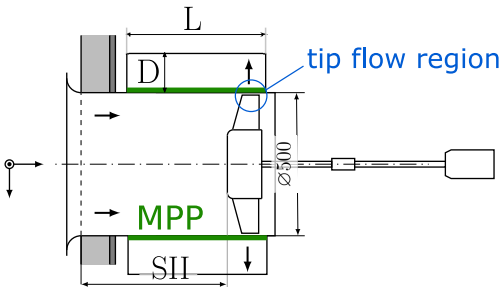

Figure 4: MPA liner arrangement with fan in position SII running above the MPP.

gion as in the substitution scenario (see Figure 7) where the fan runs inside a solid metal tube of 440 mm length and a diameter of 500 mm. The cut-on frequency of this tube is ≈ 397 Hz. The dimensions of L and D in scenario SII and SIII are the same. One must keep in mind that the expansion chamber impedance jump effect on SPL reduction diminishes as soon as higher order modes can propagate. The fans had forward (S2F) and back-

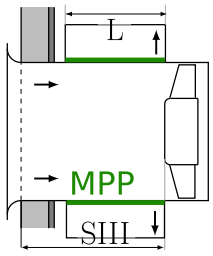

Figure 5: MPA liner arrangement with fan in position SIII running above solid metal tube section, dimension L and D same as before.

ward (S2B) skewed fan blades. This was due to the fact, that the S2B and S2F version show significantly different aerodynamic and SPL emission characteristic curves.

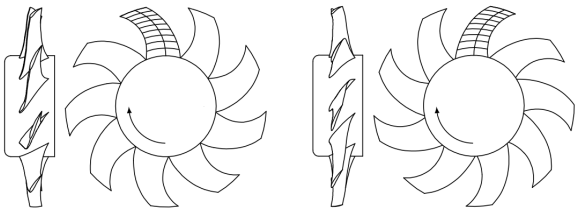

Figure 6: Forward (S2F) and backward skewed fan blades (S2B).

Experimental setup

The liner arrangement was tested at an axial fan measurement installation at iPAT (see Figure 8). The MPA section was joined to a pressure tight acoustic chamber at the suction side of the fan. The pressure difference of the chamber to ambient conditions is measured with differential pressure sensors. The flow rate is adjusted by an auxiliary fan in combination with a butterfly damper and measured via a bellmouth inlet.

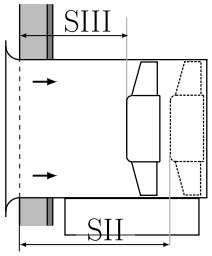

Figure 7: Investigated duct scenario with fan recessed from inflow nozzle in position SII and SIII, substitution measurement arrangement with solid metal duct tube.

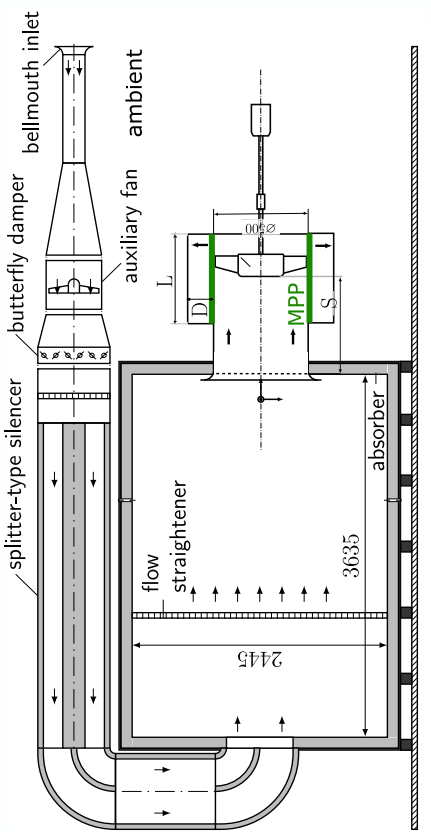

Figure 8: Axial fan measurement setup according to ISO 5801.

The emitted sound power at different operating points of the fan is assessed with microphones in horizontally and vertically lined positions (see Figure 9).

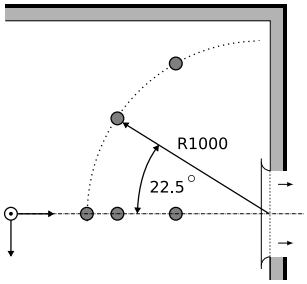

Figure 9: Microphone positioning in the test chamber covered with porous sound absorbing material, view from above.

The measured sound emissions are averaged energeti-

cally and spatially over all microphones. Then an overall sound pressure level (OSPL) and narrow band spectrum for every operating point (OP) is computed.

Results

For all following measurements results involving S2F and S2B blade geometry, the fan was rotating at 1486 RPM (rounds per minute). In the KFL (fan without blades, just grazing incident flow velocity induced by auxiliary fan) arrangement no in-stationary flow phenomena due to rotating fan blades interaction are present.

First we will evaluate the fan's efficiency meaning the ratio between flow rate multiplied by pressure difference and torque multiplied by rotational speed. In Figure 10 one can distinguish a significant efficiency drop for S2F and S2B compared to the substitution arrangement when the fans run above the MPP (SII). Nevertheless, the drop is less pronounced for S2B up to approximately 1.2 m^3s^{-1}. Changing the positioning of the fans to SIII (running above non-porous metal and same tip region size as in the substitution arrangement), eliminates this efficiency drop (see Figure 11). A slight efficiency increase is visible between a flow rate of 0.8 and 1.0 m^3s^{-1}. This

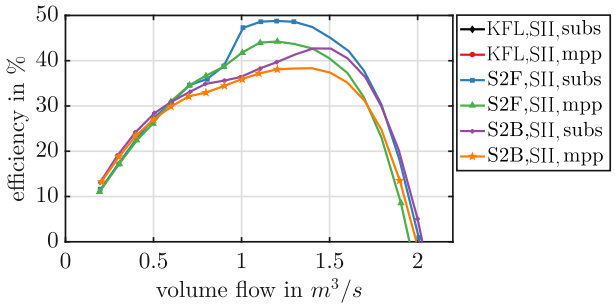

Figure 10: Fan efficiency, fan in position SII above the MPP.

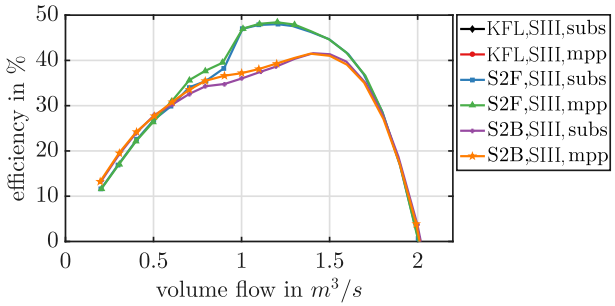

Figure 11: Fan efficiency, fan in position SIII above solid metal tube section.

slight increase in efficiency is also visible in the measured pressure difference between acoustic chamber and ambient in Figure 12. The red and black curve show that there is no significant pressure difference change when the MPP is just overflown by the fluid.

The interpretation of these two curves is that, at least, in the low Ma number cases (Ma<0.05), the MPP guides the flow in axial direction. Looking at Figure 13 reveals first that the MPA does not generate additional noise and is responsible for a constant damping of 4-6 dB at OP 1.0 m^3s^{-1} onwards. Also the MPA is much more effective for the fan in position SII if the S2B version is used. This is due to the fact, that S2F is already less loud and more efficient, so the MPA's damping effect arises less pronounced. A similar behaviour is visible in Figure 14.

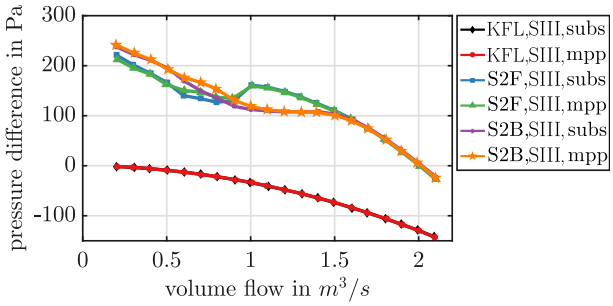

Figure 12: Pressure difference between acoustic chamber and ambient with fan at position SIII.

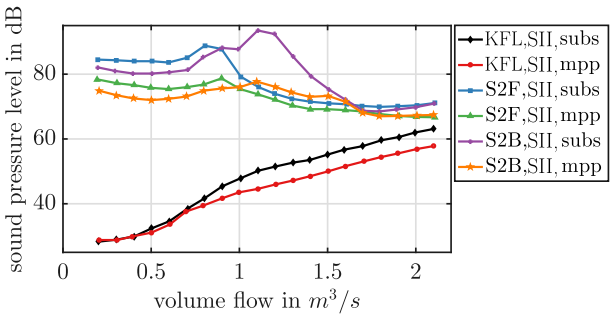

Figure 13: Overall sound pressure level (OSPL) at each operating point, fan in position SII.

The S2F curves in fan position SIII are almost identical to the ones in SII. Nevertheless, sound reduction for S2B geometry at 1.2 m^3s^{-1} is less pronounced. However, at flow rates above 1.2 m^3s^{-1} the sound reduction by the MPA is more constant and also larger for S2F and S2B, with 4-6 dB at the same scope as in the non-rotating-fan measurements (KFL). The overall sound pressure levels

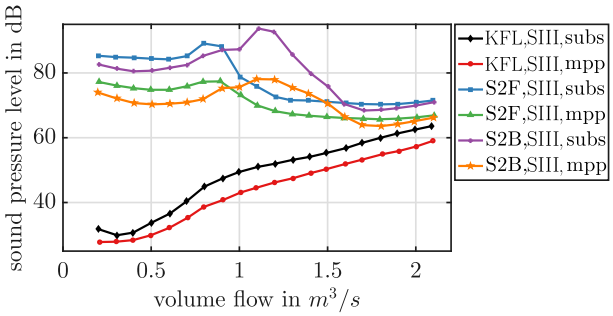

Figure 14: Overall sound pressure level (OSPL) at each operating point, fan in position SIII.

reveal only part of the MPA's damping effectiveness. One must look at the narrow band spectra at operating points to assess the absorber's impact on the desired frequency range.

This is done in the following figures. At first, when comparing with Figure 3, one can see that in comparison to near-nozzle positioning the recessed S2F fan (SII and SIII) causes the peaks at the blade passage frequency and

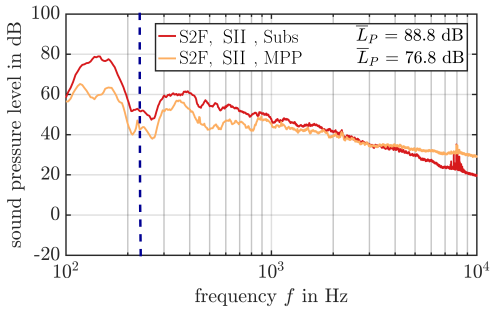

Figure 15: Narrow band spectrum at 0.8 m^3s^{-1}, SII.

its harmonics to disappear in the substitution measurement (red curves in Figures 15 and 16) for lower flow rates. The peaks reappear for higher flow rates (see Figures 17 and 18), but they are not that pronounced when compared with the near-nozzle situation (see Figure 3).
Studying Figure 15 one can see a significant reduction in sound emission below and in the range of the blade passage frequency (blue dashed line) at OP of 0.8 m^3s^{-1}. Also the range up to 1000 Hz is damped by about 8 dB. From 3000 Hz onwards we can identify the generation of additional noise not seen in the substitution measurement. A possible explanation is that the viscous shear layer above the MPP is perfused in radial direction by flow created by the fan tips. This adds anistropy to the flow field which in consequence causes additional aeroacoustic sources. If the fan runs on the non-porous metal

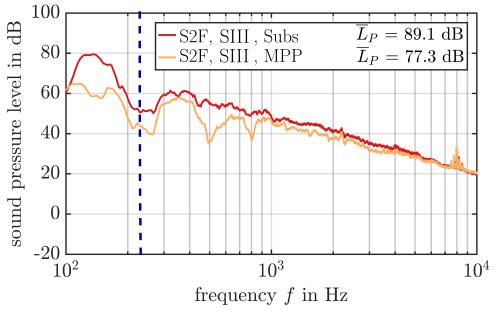

Figure 16: Narrow band spectrum at 0.8 m^3s^{-1}, SIII.

section (SIII), this effect in the spectrum above 3000 Hz is not observed (see Figure 16). One can also observe an increase in sound reduction in the range of 500 and 800 Hz. This range can be affected by changing the dimension L.
Studying Figure 17 reveals that in-stationary flow phenomena induced by the blades rotation interacting with a high stationary volume flow and the suspected perfusion of the MPP cause emission peaks at the blade passage frequency and its harmonics. The sound reduction in the range below 1000 Hz is still large, but these harmonic peaks might make the emitted sound very unpleasant to hear. Again, if the fan runs above the solid metal section, these peaks disappear(see Figure 18). In Figure 19 the spectrum at flow rate 0.9 m^3s^{-1} is depicted. This represents the unstable point in the fan's operational field. Here, additional sound due to an anistropic flow field is generated. The MPA is still effective, but

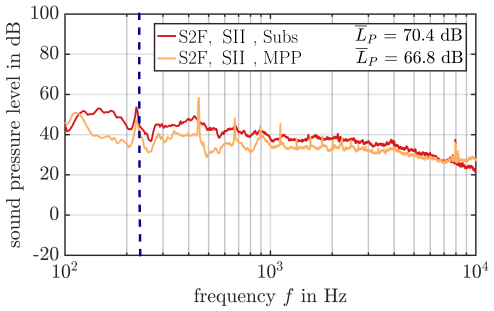

Figure 17: Narrow band spectrum at 2.0 m^3s^{-1}, SII.

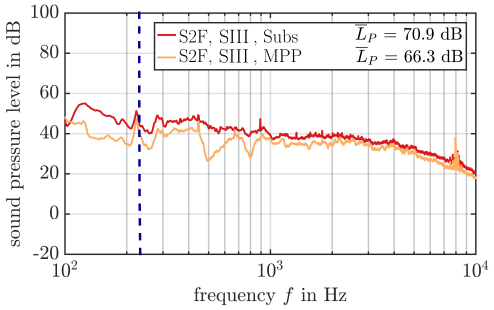

Figure 18: Narrow band spectrum at 2.0 m^3s^{-1}, SIII.

less pronounced below the blade passage frequency.

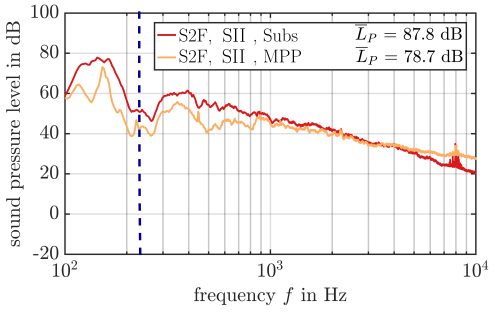

Figure 19: Narrow band spectrum at 0.9 m^3s^{-1}, SII.

Conclusion

The effects of an MPA under low Ma number flow conditions on sound emission and fan performance have been investigated. The results show the effectiveness of the absorber below 1000 Hz and that the fans's positioning above the liner absorber largely influences the fan's efficiency. There might also be additional aeroacoustic phenomena caused by the MPP's perfusion in radial direction.
Further investigations involving distorted inflow conditions and precise flow field measurements above the MPP are planned.

References

[1] Floss, S.: Different HVAC application scenarios with microperforated absorbers. DAGA proceedings (2018), 1176-1179.

[2] Krömer, F.: Sound emission of low-pressure axial fan under distorted flow conditions, Dissertation, FAU Erlangen-Nürnberg, 2018.